Journal of King Saud University – Science 35 (2023) 102445

HOSTED BY

Contents lists available at ScienceDirect

Journal of King Saud University – Science

journal homepage: www.sciencedirect.com

Original article

Geophysical evidences on reactivation of NE faults in southern Arabian Shield and its tectonic implications

Chokri Jallouli [a,*], Ali K. Abdelfattah [a], Mahmoud M. El-Waheidi [a], Saleh Alqaysi [a], Saad Mogren [a], Hassan Alzahrani [a]

[a] Department of Geology & Geophysics, King Saud University, Riyadh 11451, Saudi Arabia

ARTICLE INFO

Article history:
Received 23 February 2022
Revised 4 October 2022
Accepted 10 November 2022
Available online 15 November 2022

Keywords:
Arabian Shield
NE faults
Geophysical data

ABSTRACT

The Eastern flank of the Red sea represents an uplifted Precambrian basement that is known as the Arabian Shield. Different tectonic events were activated since the collisions among continental fragments that occurred during the period 630–550 Ma, showing very old NE ophiolite-suture zones, North trend shear zones, belts, folds, and NW Sinistral fault system known as Najd shear zones. Thus, heterogeneities and inherited faults are expected in the old basement; however, based on surface observations, NE trend faults are not described in the Arabian Shield. Despite the inconsistency with the background tectonic model of the Red Sea rifting, recent seismological studies show that active NE faults may exist in western Arabian Shield. This study aims to investigate and map the fault system in southern Arabian Shield and then better understand the tectonic system acting in the region. We provide an analysis that incorporates gravity, magnetic, and seismological data in Namas area, where earthquake sequence occurred in 2017. Using the regional-residual separation, filtering and edge detector function techniques, we identified NE trend inherited faults within the Precambrian basement that might be seismically active, as shown by the obtained distribution of epicenters and focal mechanism solutions of strike-slip style among the 2017 Namas Earthquake sequence. This result emphasizes the preexistence of a potential local tectonic process that is incongruous with the regional stress regime.

1. Introduction

Owing to complex tectonic processes, a variety of complex tectonic settings characterized the Precambrian Arabian Shield (Fig. 1) and inherent faults are suggested to be active. Seismic hazard assessments require the identification of active fault planes that produce earthquakes. Recently, the spatial distribution of earthquake hypocentres and focal mechanism solutions demarcated the NW and NE fault trends as active faults produced the earthquakes in the Al-Ays seismic dislocation zone (Abdelfattah et al., 2020; Abdelfattah et al., 2021). Furthermore, towards the south, Abdelfattah et al. (2017, 2020) suggested that the NE fault trend is the causative fault that produced the 2014 Jizan and the 2017 Namas Earthquakes.

The integrated analysis of several types of geophysical data and the application of appropriate filtering techniques are expected to be efficient in deciphering the setting of such complex tectonic structures. The Precambrian basement of the Arabian Shield shows many heterogeneities that are expressed by gravity and magnetic anomalies. Such anomalies, even though they are superimposed by other anomalies that are caused by younger structural features, they still could be distinguished and separated using adequate filtering processes. By analyzing earthquake seismic data, additional constraints on fault trends can be obtained. Therefore, the heterogeneities in basement boundaries could be mapped.

Using an integrated methodology based on the processing and interpretation of seismicity, gravity and magnetic data, this study aims to map faults and explore which of the fault planes are reactivated to produce the 2017 Namas Earthquake in the southwestern part of the Arabian Shield. The tectonic implications of obtained results are further discussed in the context of compatibility with the established tectonic system acting in the region.

* Corresponding author at: Department of Geology & Geophysics, King Saud University, Riyadh 11451, Saudi Arabia.
E-mail address: cjallouli@ksu.edu.sa (C. Jallouli).

Peer review under responsibility of King Saud University.

Production and hosting by Elsevier

https://doi.org/10.1016/j.jksus.2022.102445
1018-3647/

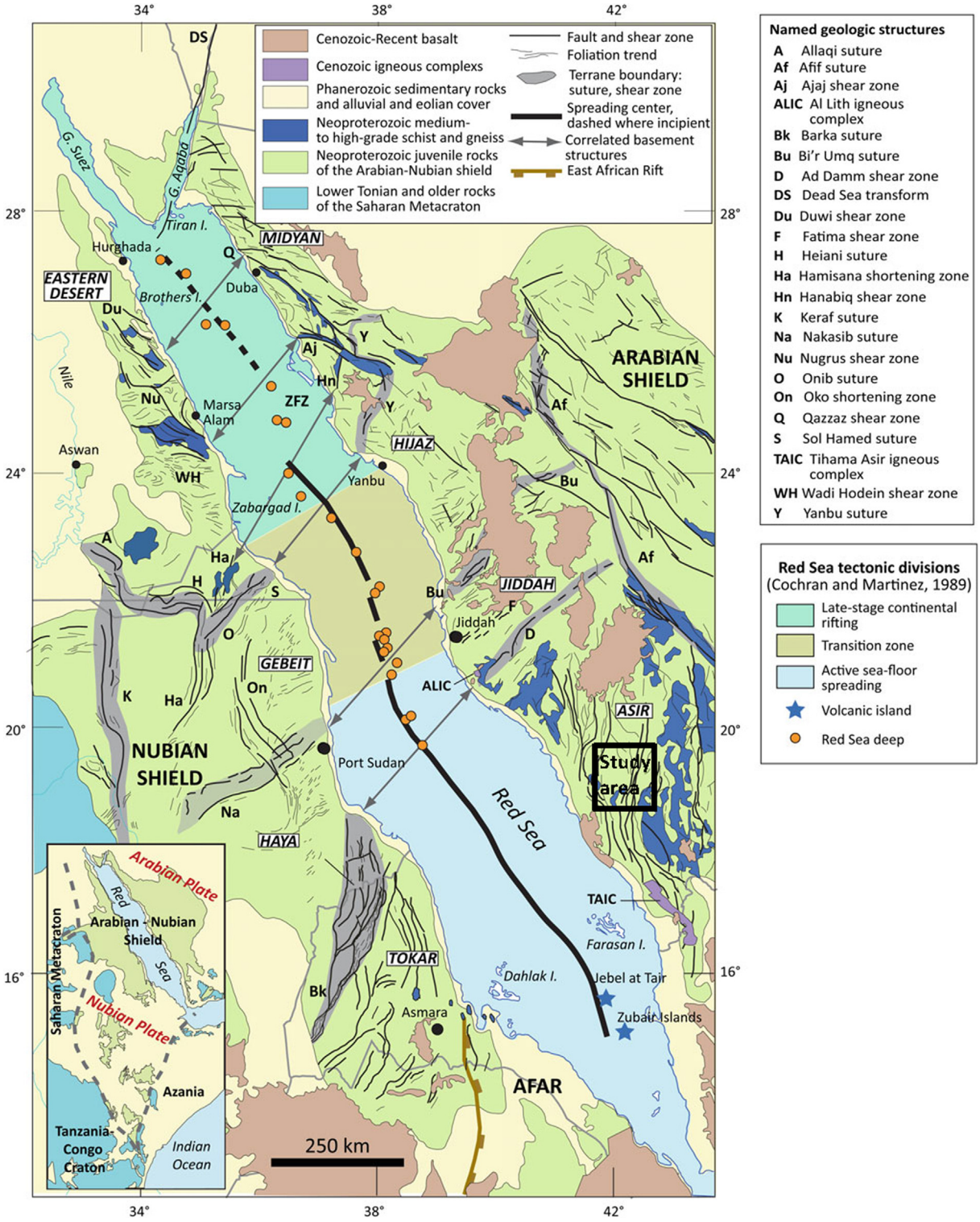

Fig. 1. Major geologic features of the Red Sea and surrounding uplifted margins of the Arabian and Nubian Shield (modified after Stern and Johnson, 2019). The black square represents location of the study area.

2. Geological setting

The Red sea flanks, where little or no sediment rocks exist, are represented by large Precambrian basement rocks (600–900 Ma) of elevation that reaches up to 2000 m or more in some localities. The basement rocks are considered as rifted continental margins and the eastern flanks are known as the Arabian Shield. The Arabian Shield is composed of granite, schist, gneiss, volcanic or sedimentary rocks. Ultramafic and ophiolitic rocks are recognized also in some localities. These uplifted Precambrian rocks are intruded by Cenozoic basalt and intrusive volcanic rocks (Fig. 1). The Arabian Shield is the result of collisions that took place among continental fragments during the period 630 Ma to 550 Ma (Stern and Johnson, 2010; Stern and Johnson, 2019). During Cenozoic, the Ara-

bian Shield is tectonically accommodated by the opening of the Red sea that was caused by a divergence movement between the African and the Arabian plates (Bosworth, 2015; Molnar et al., 2020). In the Arabian Shield, we distinguish very ancient structures represented mainly by NE ophiolite-suture zones, North-trending shear zones and NW Najd shear zones (Fig. 1). These ancient structures are resulted from the closing of the Neoproterozoic ocean basins (Abdelsalam and Stern 1996; Stern and Johnson, 2019). Furthermore, recent structures that were produced by Cenozoic divergence movements are present. These are represented by the NW trending normal faults and dykes, which are identified to be parallel to the Red Sea. Such structures are well evidenced by geophysical studies (Zahran et al., 2017; Saibi et al., 2019; Rashed et al., 2020).

Despite the numerous geophysical occurrences on the presence of NE faults in the basement structure of the Arabian platform (Stern and Johnson, 2010), no significant surface NE trending faults were reported in the Arabian Shield. Recent gravity and seismic investigations mapped NE faults in the Al-Ays area, northern Arabian Shield, (Abdelfattah et al., 2021). These faults are considered as inherited since the Proterozoic convergence tectonics and the formation of the Arabian Shield. The faults were also reactivated during the Red Sea opening. Therefore, even though NE faults are not well documented in previous geological studies due to the lack of their evident exposure at the surface, they are well evidenced by geophysical studies in the whole Arabian platform and the Arabian shield (Stern and Johnson, 2010; Abdelfattah et al. 2020; Abdelfattah et al., 2021).

3. Gravity and magnetic data analysis

3.1. Bouguer anomaly

Land gravity measurements were obtained from "Bureau Gravimétrique International (BGI)". The study area is covered by regular measurement stations with an average spacing of about 10 km. Fig. 2a shows the Bouguer anomaly of the Namas area where an earthquake of Mw 4.0 occurred in 2017. As there are seismic focuses, this area includes therefore active faults that may be revealed by gravity anomalies if these faults induce density contrasts.

Furthermore, long and short wavelengths are revealed on the Bouguer anomaly map; these are attributed to a contrast in the density of the subsurface rocks. The amplitude has a general increase from – 130 mGal to 10 mGal toward the Red sea. To emphasize the occurrence of these anomalies that originated by shallow sources, we proceeded to separate the observed Bouguer anomalies into regional and residual. As we have no information on deep sources that caused the long-wavelength anomalies in the studied area, we removed a smooth polynomial surface from the observed Bouguer anomalies using the method proposed by Gabtni and Jallouli (2017). The obtained residual anomalies (Fig. 2b) in the study area are the result of density contrasts, such as those in the Precambrian basement, dykes, or faults. As the average spacing between gravity stations is 10 km, all wavelengths lower than 20 km are not reliable, so we applied a low pass filter that cuts wavelengths of less than 20 km. This filter preserves all prominent residual anomalies but they become smoother (Fig. 2b).

The dominating residual gravity anomalies are trending in the NE direction, which is not common in the area, and it is not reported in the geologic literature that dealt with the surface geology of the investigated area. The width of the anomalies is less than 40 km with an amplitude of 10 to 20 mGal and an extent range 50–100 km (Fig. 2b). Taking into account the geological setting of the study area, these gravity NE-trending anomalies are attributed to the Precambrian basement structure of the Arabian Shield.

3.2. Magnetic anomalies

Magnetic data processing was conducted using the Global magnetic anomaly EMAG2 (Maus et al., 2009; Meyer et al., 2017). The process consists of a merged grid compiled from all available magnetic measurements and represents the total magnetic anomalies at 4 km above geode in 2 arc-minutes resolution. Using EMAG anomalies, it is possible to constrain the main structures and composition of the crust. Figure-3a shows the total magnetic anomalies of the study area, which reveal a magnetic intensity variation in the range of −140 to 90 nT. Furthermore, it can be noticed that there are several positive and negative anomalies that extend in different directions. Anomalies occur because of the magnetic heterogeneities in the basement rocks that result from variations in the composition of magnetic rocks, or because of inherited faults that affect the basement rocks. To reduce the complexity in the shape of the observed anomalies, we reduced the observed anomalies to a pole by applying the RTP filter using GMT software (grdredpol module). This process is applied assuming that the field and magnetization vectors are collinear. Declination and inclination at each point are computed from IGRF2000. Although the RTP filter could not be applied efficiently to all anomalies, it still can remove an order of complexity and replaces induced anomalies over their sources. Further, since we are not interested in small sources, for instance local heterogeneities or small structures, we have applied a low pass filter to remove short wavelengths. The applied filter cut out the wavelengths of less than 20 km, the same cut-off is used for gravity anomalies. The filtering process produced smoothed anomalies with high amplitudes of hundreds of nT that are trending in different directions (Fig. 3b). The obtained anomalies are caused by major magnetic heterogeneities within the basement in the study area that could be induced by inherited faults.

3.3. Boundary analysis of gravity and magnetic anomalies

Gravity and magnetic anomalies in the study area are associated with basement heterogeneities of the Arabian Shield. The heterogeneities result from the arrangement of different basement blocks that are varied in their compositions and densities. The edges of such blocks are bounded by inherited faults that have resulted from collisions between continental fragments of crust that occurred during the period 630–550 Ma (Stern et al., 2010).

For the purpose of locating the basement heterogeneities and faulting in the Arabian Shield, we analyzed anomalies in gravity and magnetic field using edge detector filters. The method has been employed by several authors to investigate rock heterogeneities and faults (Jallouli and Mickus, 2000; Jallouli et al., 2013; Saibi et al., 2019). Among these techniques, the horizontal gradients of potential field anomalies which is considered an efficient technique to detect basement blocks' boundaries that have different densities or magnetic properties. The process permits the location of the edge of sources, faults, dykes, or any basement heterogeneity implying density or magnetic susceptibility contrast. In our work, the Magnitude of the Horizontal Gradient (MHG) method (Eq. (1)) was used to locate the edges of the crustal block.

$$\mathrm{MHG}\,(x,y) = \sqrt{\left(\frac{\partial U}{\partial x}\right)^2 + \left(\frac{\partial U}{\delta y}\right)^2} \quad (1)$$

where.

$\left(\frac{\partial U}{\partial x}\right)^2$ and $\left(\frac{\partial U}{\partial y}\right)^2$ indicates the horizontal gradients of the potential field (U) along x and y directions, respectively.

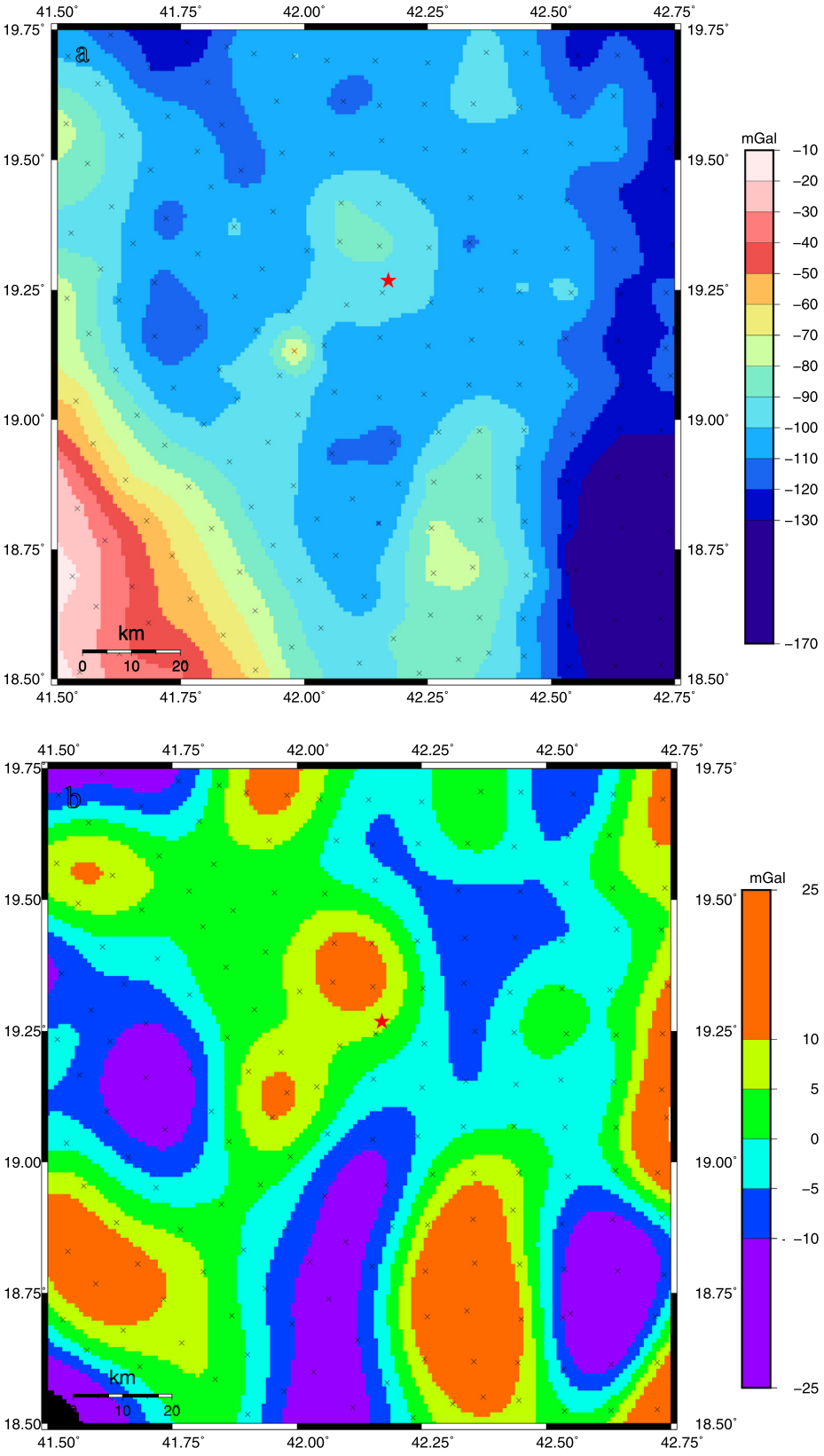

Fig. 2. (a) Complete Bouguer anomaly map of the study area derived from data obtained from BGI. (b) Residual anomaly map obtained after extraction of a smooth polynomial surface from the observed Bouguer anomalies and low-pass filter cutting wavelength of less than 20 km. Crosses represent locations of gravity stations, contour interval is 10 mGals. Red star refers to the epicenter of the main shock of 2017 Namas earthquake.

Peaks or maxima of MHG delineate edges of the crustal blocks with different densities or magnetic properties. The MHG of the residual gravity anomaly reveals the gravity trends caused by basement heterogeneities implying density contrasts (Fig. 4a). The

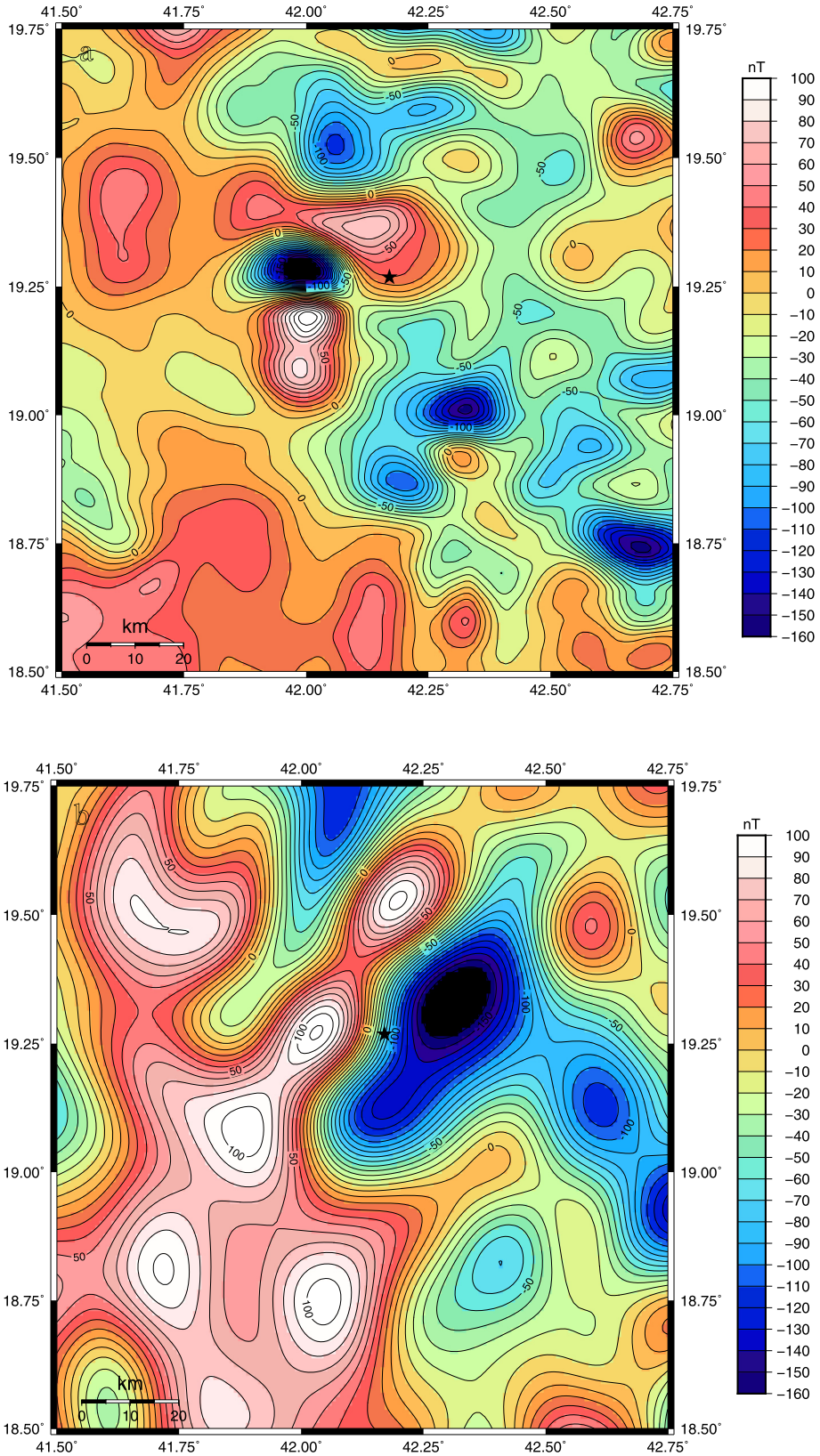

Fig. 3. (a) Total magnetic anomaly map of the study area derived from EMAG2. This map shows all magnetic anomalies caused by the basement rock heterogeneities including induced and remnant anomalies. (b) Total magnetic anomalies map reduced to pole and smoothed by a low-pass filter cutting wavelength less than 20 km. Contour interval is 10 nT. Black star refers to the epicenter of the main shock of 2017 Namas earthquake.

MGH of the RTP magnetic anomaly reveals the magnetic trends caused by basement heterogeneities implying magnetic property contrasts (Fig. 4b). These trends mainly correspond to the edges of the crustal blocks induced by inherited faults.

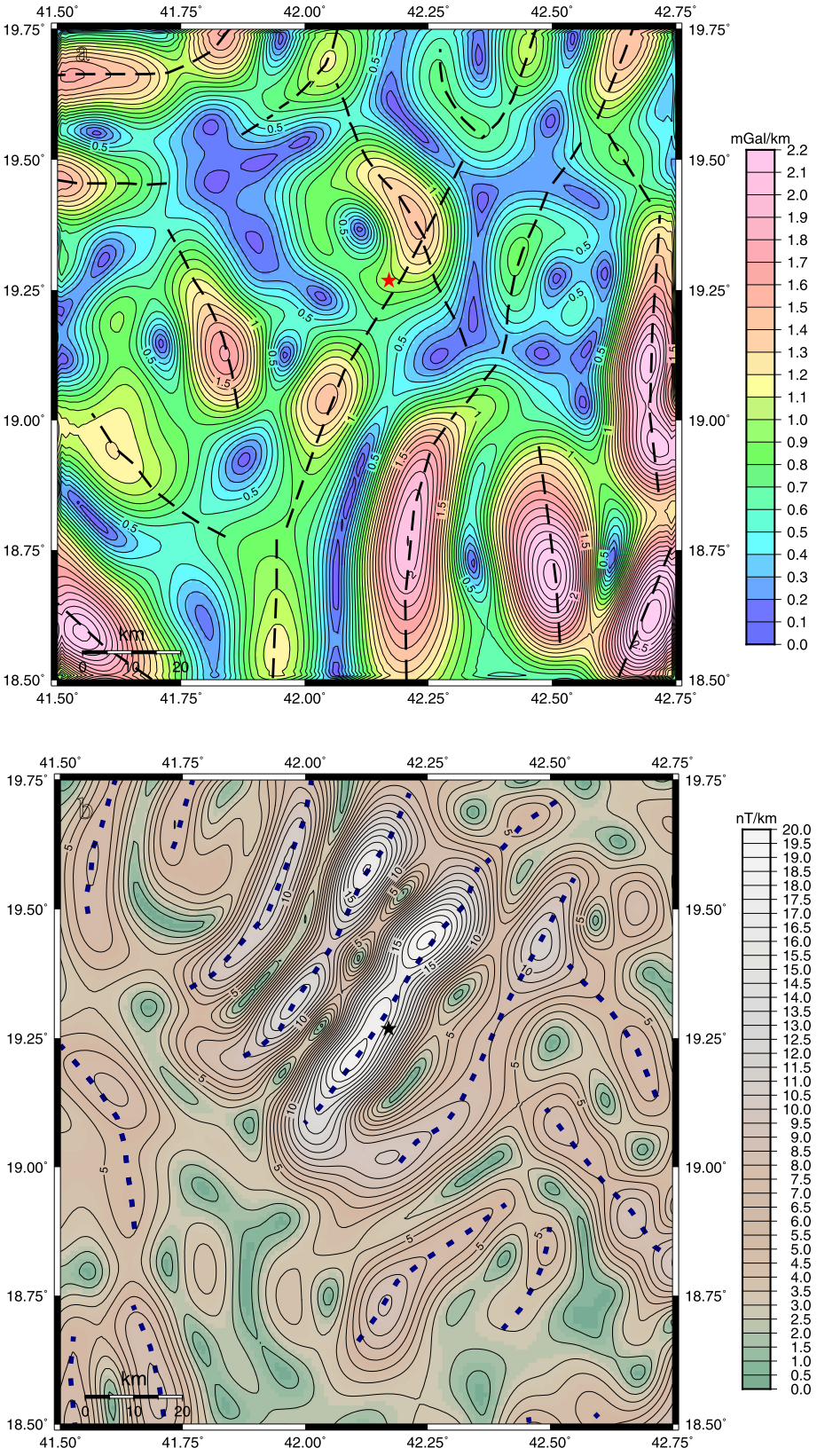

Fig. 4. (a) Map of the Magnitude of horizontal gradient (MHG) derived from the residual gravity anomalies. It shows the gravity lineaments that correspond to edge locations of density contrasts within blocks of the basement of the Arabian Shield. Contour interval is 0.1 mGal/km. (b) Map of the Magnitude of horizontal gradient (MHG) derived from the RTP magnetic anomalies. It shows the magnetic lineaments that correspond to edge locations of magnetic property contrasts within blocks of the basement of the Arabian Shield. Contour interval is 1 nT/km. Star refers to the epicenter of the main shock of 2017 Namas earthquake.

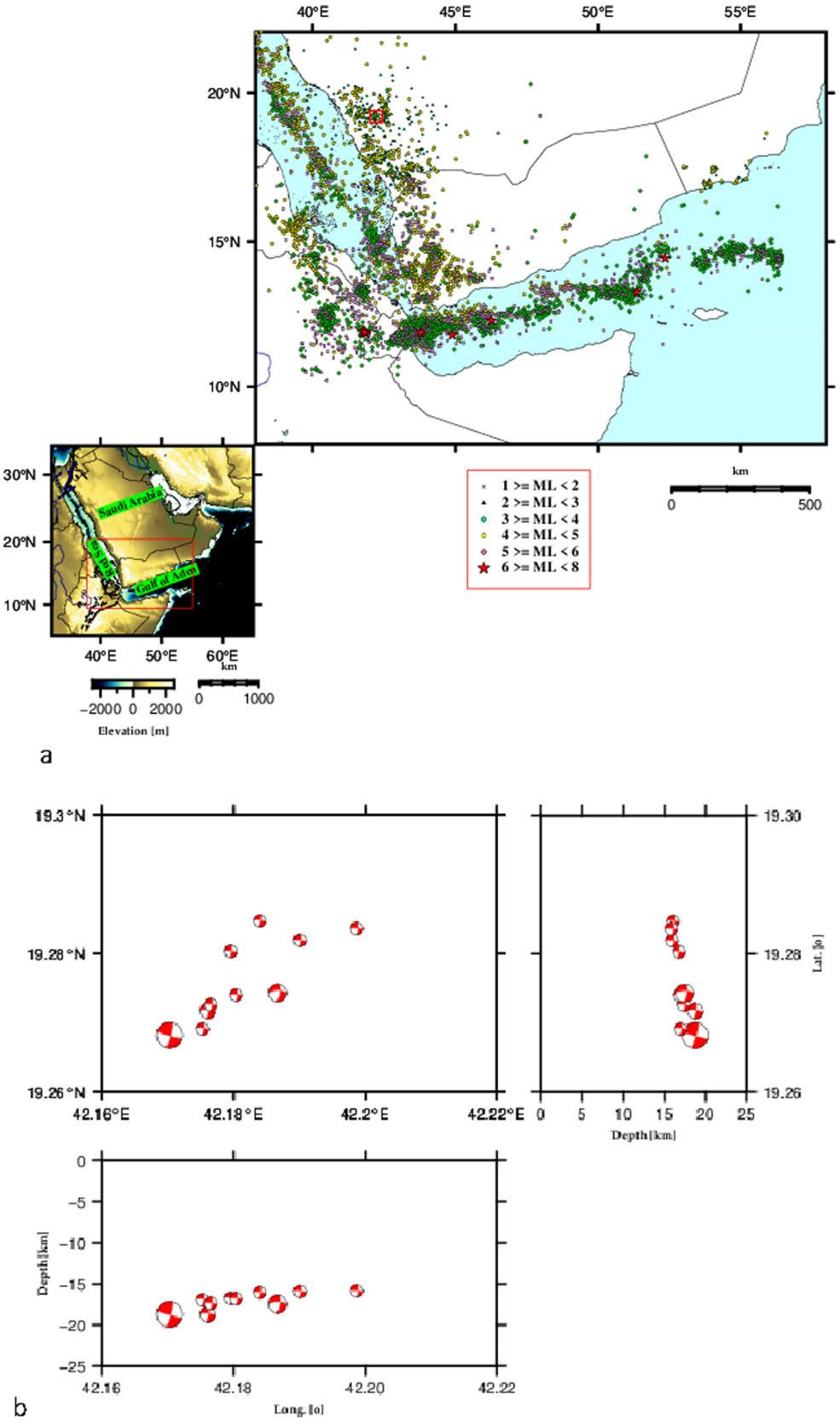

Fig. 5. (a) The spatial distribution of earthquakes that occurred in the southern Red Sea region for the period of 1962–2020. The distribution of earthquakes was projected in terms of magnitude, latitude and longitude. Square represent location of Namas area. (b) The spatial distribution of the focal mechanism solutions for the events of Mw $\geq$ 2.0 among the 2017 Namas earthquake sequence. The distribution was illustrated in terms of magnitude, latitude and longitude. The largest beach ball represents the focal mechanism solution of the mainshock that exhibited a dextral strike-slip displacement along the NE-SW faulting trend.

4. Seismicity and focal mechanism solutions

The earthquake location parameters were collected from several sources, which are Ambraseys (1988), Ambraseys et al. (1994), the Centre of Seismic Studies at King Saud University, the Seismographic Network of King Abdulaziz City of Science and Technology, the Saudi Seismographic National Network (SSNN) of the Saudi Geological Survey, and the Seismological International Centre. Figure-5a shows the seismicity in the region during the period 1900–2021. According to Figure-5a, the epicenters of the earthquakes are distributed in the axial rift along the Red Sea, Gulf of Aqaba, and Afar region. However, the seismicity also extends to the Red Sea's eastern and western flanks. Along the eastern Red Sea flank, the seismicity is randomly distributed where fault trends can be demarcated from the distribution of epicenters. The random distribution of epicenters can be attributed to the low resolution of locations before the installation of the SSNN. Recently, and following the installation of SSNN, the 2017 earthquake sequence that occurred in the study area was examined by Abdelfattah et al. (2020) to resolve high-resolution earthquake relocation and focal mechanism solutions. The 2017 Namas earthquake occurred at 01:06 universal times on 03 Nov. 2017. Its seismic moment of 1.12E + 15 Nm is equivalent to a Mw of 4.0 (Abdelfattah et al. 2020).

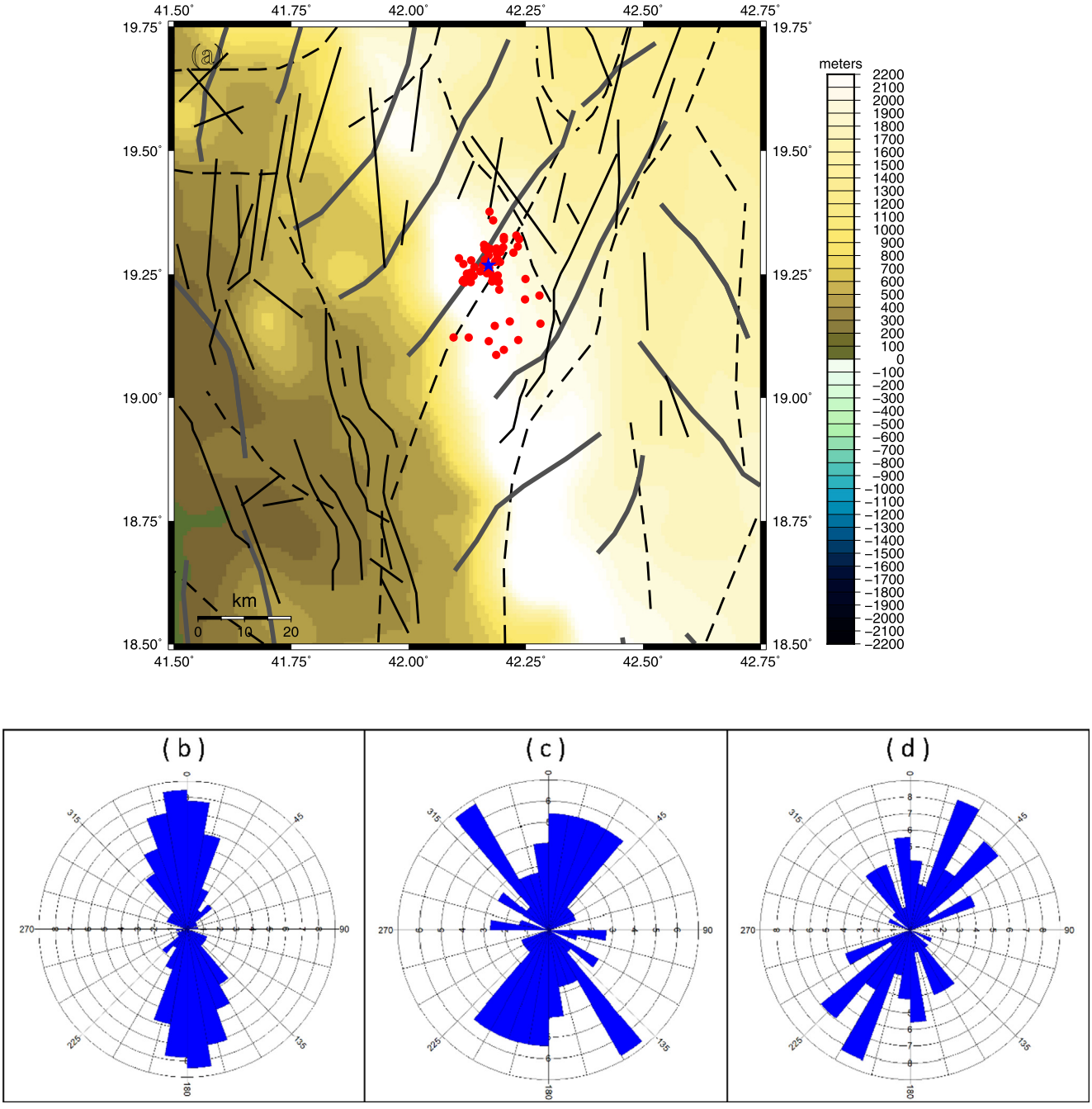

Fig. 6. (a) Structural map showing gravity and magnetic trends that were obtained from the MHG (Fig. 4), surface observed faults mirrored from the geological map and seismic epicenters with magnitude higher than 2.0. Thin black lines represents surface observed faults, dashed black lines represents gravity trends shown in figure-4a, gray thick lines represent magnetic trends shown in figure-4b. The Blue star refers to the epicenter of the main shock of 2017 Namas earthquake. (b), (c) and (d) are rose diagrams showing direction frequency of surface, gravity and magnetic trends respectively.

The quantity of high-quality data from the 2017 Namas earthquake provides an unusual impute to examine the source characteristics of the events with an Mw greater than 2.0. Figure-5b shows the distributions of focal mechanism solutions of the 2017 earthquake sequence. The hypocenter distributions along the latitude and longitude are also displayed. The figure illustrates the spatial distribution of earthquakes in terms of focal depth, magnitude, latitude and longitude. The distribution demarcated the NE-SW direction that is approximately parallel to the fault plane solutions for the events of moment magnitude greater than 2.0; this indicates a fault system of dextral strike-slip mechanisms. The fault plane parameters of the mainshock earthquake are 27°, 61° and −144° in the strike, dip and rake, respectively. The fault plane solutions showed that the earthquake has resulted from a right-lateral shear slip over a segment of the preexisting NE fault trends in the region, which conjugate to the NNW fault trends parallel to the axial fault in the Red Sea.

5. Results and discussion

The Arabian Shield is an uplifted Precambrian basement and represents the Eastern flank of the Red sea. As an old shield, its structure has been under many tectonic events since the convergence and collisions among continental fragments that occurred during the period 630–550 Ma. As a result of the different tectonic events, the Arabian Precambrian Shield shows very old NE ophiolite-suture zones, North trend shear zones, belts, folds, NW sinistral fault system known as Najd shear zones (Fig. 1) and NW-SE strike extensional faults that runs parallel to the Red Sea spreading axis. Hence, the presence of heterogeneities and inherited faults is expected.

Using a suitable edge detector function, we mapped the gravity and magnetic trends (Fig. 2 and Fig. 3). It was found that different basement boundaries that trending in various directions were successfully mapped by gravity and magnetic analysis. However, the NE trending faults are the most dominant and well delineated implying a heterogeneous distribution of densities and magnetic susceptibility within the basement. There are significant complementary findings between gravity and magnetic results. Indeed, magnetic anomalies well delineate some trends that are not visible on the gravity anomaly maps. These trends represent the main faults and boundaries within the basement that induced a density or magnetic properties contrasts. Gravity and magnetic trends are integrated with surface observed faults and seismic epicenters in one map (Fig. 6a). This map deciphers clearly the presence of prominent NE faults or basement boundaries. Besides, the focal mechanism solutions of the seismic activity occurred in 2017 reveal a dextral active NE strike slip fault (Fig. 5). To further evaluate how well the NE trends are represented in the study area, rose diagrams representing the frequency of surface, gravity and magnetic trends are drawn (Fig. 6b). Surface observation-based diagrams confirm that all trends are in the N—S direction, whereas rose diagram of gravity and magnetic trends show, in addition to NW direction, a high frequency of NNE to NE trends.

In this study, an integrated approach that based on surface observations and geophysical findings were implemented. Even though the NE trends are not observed on the surface, they are well mapped by geophysical studies. In addition, if we consider the spatial distribution of epicenters, it appears they are trending along NE around trends detected by gravity and magnetic analysis as well. As the Arabian Shield is actually under the regional extension related to the Red sea spreading that should be associated with NW faults, the NE trending faults evidenced by gravity, magnetic and seismic data are therefore inherited. Indeed, the Arabian Shield subjected to numerous tectonic stages and, thus, its structure is largely resulted by old collisions between continental fragments, which have left behind many inherited faults, and heterogeneities. Therefore, the interpretation of the NE trending gravity anomalies to be caused by inherited NE faults and the variations in composition and densities within the Precambrian basement seems to be solid and justified.

Although the NE faults have not been well documented in previous geological studies, possibly because they are not readily visible at surface, geophysical studies in the Arabian platform (Stern and Johnson, 2010) and northern Arabian shield (Abdelfattah et al., 2021) have confirmed the existence of these faults. Further, focal mechanism solutions of the 2014 and the 2017 earthquakes that took place in the southern Arabian exhibited a comparable focal mechanism solution of dextral shear slip over the NE fault trend (Abdelfattah et al. 2017; Abdelfattah et al. 2020). Therefore, NE faults exist in the whole Arabian plate and they could be reactivated. As the Arabian plate is currently moving toward the NNE and the Red Sea is spreading, this causes an extensional stress and a rejuvenation of pre-existed NE faults in the Precambrian basement as a strike-slip fault, implying a local tectonic setting that could be different from the large-scale regional stress. The Namas earthquake sequence seems incompatible with the current knowledge of the ambient tectonics of the region imported by the active geodynamic process associated with the Red Sea rifting. In the Arabian shield, NW normal faults are impacted by active rifting in the Red Sea, while a dextral fault style represents a reemergence of an old fault buried in the old Precambrian basement.

6. Conclusion

In this study, we have integrated gravity, magnetic, and seismological data to identify the active fault system that is believed to cause the recent seismic activity in the southwestern Arabian Shield. Using multiple-stage processes including regional-residual separation, filtering and edge detector function, we identified the main gravity and magnetic trends that correspond to the main basement heterogeneities caused by variation in density and magnetic properties. Focal mechanism solutions and epicenters spatial distribution were integrated with gravity and magnetic anomalies to draw out the following conclusions:

- Despite they are not described based on surface observations, NE trending faults exist in the southern Arabian Shield and they may be active.
- The NE trending faults resolved from the analysis of gravity and magnetic data suggests the existence of inherited-fault types that are buried in the basement and could have recently generated seismicity.
- Due to the Red sea opening, the present-day tectonic stress is related to the movement of the Arabian plate toward the NNE direction, indicating a rejuvenation of the pre-existed NE strike-slip faults in the Precambrian basement.
- Considering the distribution of relocated epicenters, focal mechanism solutions, and gravity and magnetic anomalies, the fault that caused the 2017 Namas earthquake sequence runs in the NE-SW direction that is inconsistent with the tectonic in the region. The study area in southern Arabian Shield is a case where the local tectonic setting is different from the large-scale regional stress.

Declaration of Competing Interest

The authors declare that they have no known competing financial interests or personal relationships that could have appeared to influence the work reported in this paper.

Acknowledgement

This research was supported by Researchers Supporting Project number (RSP2022R432), King Saud University, Riyadh, Saudi Arabia.

We are grateful to the "Bureau Gravimétrique International (BGI)" for providing the gravity data. The software, Generic Mapping Tools developed by Wessel and Smith (1998), was used for data processing and mapping.

Appendix A. Supplementary material

Supplementary data to this article can be found online at https://doi.org/10.1016/j.jksus.2022.102445.

References

Abdelfattah, A.K., Al-Amri, A., Abd el-aal, A.K., Zaidi, F.K., Fnais, M., Almadani, S., Al-Arifi, N., 2017. The 23 January 2014 Jizan earthquake and its tectonic implications in southwestern Saudi Arabia. Tectonophysics 712, 494–502.

Abdelfattah, A.K., Al-amri, A., Soliman, M.S., Zaidi, F.K., Qaysi, S., Fnais, M., Almadani, S., Al-Arifi, N., 2020. An analysis of a moderate earthquake, eastern flank of the Red Sea, Saudi Arabia. Earth Planets Space 72 (1), 1–17.

Abdelfattah, A.K., Jallouli, C., Fnais, M., Qaysi, S., Alzahrani, H., Mogren, S., 2021. The key role of conjugate fault system in importing earthquakes into the eastern flank of the Red Sea. Earth, Planets Space 73 (1), 1–19.

Abdelsalam, M.G., Stern, R.J., 1996. Sutures and shear zones in the Arabian-Nubian Shield. J. Afr. Earth Sc. 23 (3), 289–310.

Ambraseys, N.N., Menu, J.A.M., 1988. Earthquake-induced ground displacements. Earthquake Eng. Struct. Dyn. 16 (7), 985–1006.

Ambraseys, N.N., Srbulov, M., 1994. Attenuation of earthquake-induced ground displacements. Earthquake Eng. Struct. Dyn. 23 (5), 467–487.

Bosworth, W., 2015. Geological evolution of the Red Sea: historical background, review, and synthesis. In: The Red Sea. Springer, Berlin, Heidelberg, pp. 45–78.

Gabtni, H., Jallouli, C., 2017. Regional-residual separation of potential field: an example from Tunisia. J. Appl. Geophys. 137, 8–24.

Jallouli, C., Mickus, K., 2000. Regional gravity analysis of the crustal structure of Tunisia. J. Afr. Earth Sc. 30 (1), 63–78.

Jallouli, C., Mogren, S., Mickus, K., Turki, M.M., 2013. Evidence for an east–west regional gravity trend in northern Tunisia: Insight into the structural evolution of northern Tunisian Atlas. Tectonophysics 608, 149–160.

Maus, S., Barckhausen, U., Berkenbosch, H., Bournas, N., Brozena, J., Childers, V., Dostaler, F., Fairhead, J.D., Finn, C., Von Frese, R.R.B., Gaina, C., 2009. EMAG2: A 2–arc min resolution Earth Magnetic Anomaly Grid compiled from satellite, airborne, and marine magnetic measurements. Geochem. Geophys. Geosyst. 10 (8).

Meyer, B., Saltus, R., Chulliat, A., 2017. EMAG2: Earth magnetic anomaly grid (2-arc-minute resolution) version 3. National Centers for Environmental Information, NOAA. Model. doi, 10, p.V5H70CVX.

Rashed, M., Zahran, H., Atef, A., Harbi, H., Al-Dhahry, M., Al-Hady, S., 2020. A new perspective of the 2009 Al-Ays earthquake episode at western Arabia. J. Asian Earth Sci. 188, 104101.

Saibi, H., Mogren, S., Mukhopadhyay, M., Ibrahim, E., 2019. Subsurface imaging of the Harrat Lunayyir 2007–2009 earthquake swarm zone, western Saudi Arabia, using potential field methods. J. Asian Earth Sci. 169, 79–92.

Stern, R.J., Johnson, P., 2010. Continental lithosphere of the Arabian Plate: a geologic, petrologic, and geophysical synthesis. Earth Sci. Rev. 101 (1–2), 29–67.

Stern, R.J., Johnson, P.R., 2019. Constraining the opening of the Red Sea: Evidence from the Neoproterozoic margins and Cenozoic magmatism for a volcanic rifted margin. In: Geological Setting, Palaeoenvironment and Archaeology of the Red Sea. Springer, Cham, pp. 53–79.

Zahran, H.M., El-Hady, S.M., Abuelnaga, H.S., 2017. Aeromagnetic data over Harrat Lunayyir and surrounding areas, western Saudi Arabia. Arabian J. Geosci. 10 (3), 1–15.

Further reading

Wessel, P., Smith, W.H., 1998. New, improved version of Generic Mapping Tools released. Eos, Trans. Am. Geophys. Union 79 (47), 579.